

pubs.acs.org/JPCB Article

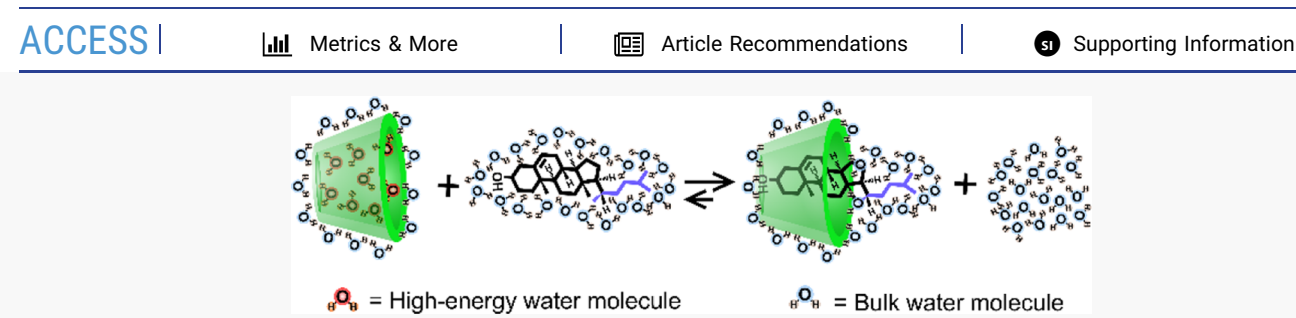
Measurement of Single-Molecule Forces in Cholesterol and Cyclodextrin Host-Guest Complexes

Shankar Pandey, Yuan Xiang, Dilanka V. D. Walpita Kankanamalage, Janarthanan Jayawickramarajah, Yongsheng Leng, and Hanbin Mao*



Cite This: J. Phys. Chem. B 2021, 125, 11112–11121





ABSTRACT: Biological host molecules such as β-cyclodextrins (β-CDs) have been used to remove cholesterol guests from membranes and artery plaques. In this work, we calibrated the host–guest intermolecular mechanical forces (IMMFs) between cholesterol and cyclodextrin complexes by combining single-molecule force spectroscopy in optical tweezers and computational molecular simulations for the first time. Compared to native β-CD, methylated beta cyclodextrins complexed with cholesterols demonstrated higher mechanical stabilities due to the loss of more high-energy water molecules inside the methylated β-CD cavities. This result is consistent with the finding that methylated β-CD is more potent at solubilizing cholesterols than β-CD, suggesting that the IMMF can serve as a novel indicator to evaluate the solubility of small molecules such as cholesterols. Importantly, we found that the force spectroscopy measured in such biological host–guest complexes is direction-dependent: pulling from the alkyl end of the cholesterol molecule resulted in a larger IMMF than that from the hydroxyl end of the cholesterol molecule. Molecular dynamics coupled with umbrella sampling simulations further revealed that cholesterol molecules tend to enter or leave from the wide opening of cyclodextrins. Such an orientation rationalizes that cyclodextrins are rather efficient at extracting cholesterols from the phospholipid bilayer in which hydroxyl groups of cholesterols are readily exposed to the hydrophobic cavities of cyclodextrins. We anticipate that the IMMF measured by both experimental and computational force spectroscopy measurements help elucidate solubility mechanisms not only for cholesterols in different environments but also to host–guest systems in general, which have been widely exploited for their solubilization properties in drug delivery, for example.

■ INTRODUCTION

The solubility of cholesterol in different environments is of high physiological importance as it is involved in many physiological and pathological processes. For instance, in atherosclerosis, the slightly soluble cholesterol in the blood stream is the cause for cholesterol crystal formation in artery plaques. In lipid rafts, cholesterols are enriched, a result of its preferential solubility in these heterogenous membrane domains.^{2,3} To deplete cholesterols in both artery plaques and lipid membranes, bio-host molecules such as cyclodextrins and their derivatives have been used. 4-6 It has been shown that native β -cyclodextrin (β -CD) and derivatives can reduce the cholesterol content in cells or virus membranes for potential antivirus therapies.⁷ In addition, cyclodextrins have also been used to enrich the cholesterol content in the membrane of tissue culture cells.8-10 The efficiency of the cholesterol enrichment or depletion is governed by the solubility of the cholesterol in cyclodextrins with respect to specific environThe solubility of a chemical is traditionally determined by the intermolecular force (IMF)⁷ between the chemical and the solvent. However, IMF is a thermodynamic parameter that has been frequently characterized by the chemical energy required to disassemble a particular intermolecular interaction. As a thermodynamic parameter, IMF does not contain the information relevant to the molecular force direction or assembly/disassembly pathways for intermolecular interactions. Consequently, it cannot reflect the kinetic solubilization processes which are closely dependent on the direction as well as the pathway of intermolecular interactions^{11,12} between solutes and solvents.

Received: May 1, 2021 Published: September 15, 2021





In this work, we directly measured the intermolecular mechanical force (IMMF) between cholesterol and cyclodextrin in a host-guest complex at the single-molecule level. In contrast to the IMF, which is a thermodynamic term, IMMF evaluates mechanical strength between molecular interactions and therefore, is a kinetic term that reflects the pathway and orientation effect on these interactions. We used singlemolecule rupture force measurements in optical tweezers, in combination with computational force spectroscopy simulations, to calibrate mechanical forces required to disassemble the cholesterol-cyclodextrin host-guest complexes from two opposite orientations, that is, pulling from the hydroxyl head group and that from the alkyl tail of the cholesterol molecules. For free cholesterols in solution, either end of a cholesterol molecule has the chance to interact with a cyclodextrin molecule. In phospholipid bilayer membranes, however, it is the hydroxyl head of the cholesterol that interacts with the cyclodextrin first. 13 The interaction strength from such a direction can be evaluated by the disassembly of the cholesterol-cyclodextrin complex from the alkyl tail. Previously, atomic force microscopy (AFM)^{14,15} has been used to study the mechanical interaction strength of host-guest complexes. However, AFM has limitations including the nonspecific interaction between the AFM tip and sample. It also suffers from the lower bound of the useful force range to probe molecular interactions. 16 The orientational effect of guest molecules in a host molecule has been analyzed with NMR^{17-19} at the ensemble average level; here, we show that cholesterol guest orientations in cyclodextrin complexes can be analyzed at a single-molecule level in our IMMF measurements in optical tweezers. All the mechanical disassembly experiments were simulated by nonequilibrium steered molecular dynamics (SMD) simulations 20-23 to establish relevant singlemolecule force spectroscopy distributions, which showed striking agreement with the optical-tweezer IMMF results. Our combined experimental and computational simulation studies provide molecular insights into the solubility property of cholesterol in cyclodextrins, which are not attainable merely based on mechanical unfolding experiments or computational simulations on cholesterol-cyclodextrin interactions. 24-26 The IMMF revealed by combined experimental and computational force spectroscopies can be readily extended to understand other intermolecular interactions such as host-guest systems, in which the solubility of the guest molecules in host cavities is a critical consideration for their wide applications.²⁷,

■ MATERIALS AND METHODS

General Experimental Section. DNA oligos were purchased from the Integrated DNA Technologies (IDT, IA). Enzymes were purchased from New England Biolab (NEB, Ipswich, MA) for the preparation of DNA constructs. Streptavidin or anti-digoxigenin-coated polystyrene bead were purchased from Spherotech (Lake Forest, IL). Azide-modified native β -CD and azide-modified permethylated β -cyclodextrin (Me- β -CD) were prepared according to the literature.²⁹ Azidopropyl DNA was synthesized by coupling amino-modified DNA with 4-azidobutyrate NHS-ester, according to a literature procedure previously developed in our groups, 30 Azido-TEG (triethylene glycol)-cholesterol and 27-alkyne cholesterol were purchased from Sigma Aldrich and Click Chemistry Tools, respectively. Unless otherwise stated, all chemicals and solvents were purchased from Sigma-Aldrich or Fisher Scientific $(\geq 99\%)$ and used without further purification.

Synthesis of *β*-**CD-DNA.** A solution of 8 μ L (250 μ M) of azide-modified β -CD and 2 μ L (250 μ M) of hexynyl-modified DNA were taken in an Eppendorf tube. Then, 3 μ L of click solution containing 1 μ L of CuBr solution (0.01 g of CuBr in 700 μ L of DMSO/t-BuOH in 3:1) and 2 μ L of Tris[(1-benzyl-1H-1,2,3-triazol-4-yl)methyl]amine (TBTA) ligand solution were treated in the tube. The reaction mixture was purged with N₂ gas and shaken for 14 h in the dark at room temperature. To remove unreacted reactants from the click reaction mixtures, ethanol precipitation was performed, and the precipitant was dissolved in 15 μ L of water. The click product was analyzed with a 15% denaturing polyacrylamide gel electrophoresis (PAGE) gel (Figures S1 and S2). Then, 15% denaturing PAGE gel was used to purify the upper band (see Figure S3 for the purified product).

Synthesis of Me-\beta-CD-DNA. A solution of 1 mg (0.8 μ mol) of azide-modified Me- β -CD in 100 μ L of H₂O was added to an Eppendorf tube containing 0.1 μ mol hexynylmodified DNA in 100 μ L of H₂O. In a separate vial, 15 μ L of CuBr solution (100 mM in DMSO/tBuOH 3:1) and 30 μ L of TBTA ligand solution (100 mM in DMSO/tBuOH 3:1) were vortexed and added to the DNA + Me- β -CD-N₃ solution. The solution was shaken at room temperature for 3 h. A G25 microspin-column was used for desalting. The Me- β -CD -DNA conjugate was purified by RP-high-performance liquid chromatography, and the structure was confirmed by matrix-assisted laser desorption ionization time-of-flight (Figures S1 and S4).

Synthesis of 3' Cholesterol-Propyl-DNA. A solution of 2 μ L (250 μ M) of azido-propyl-modified DNA was mixed with 8 μ L (250 μ M) of 27-alkyne cholesterol. Then, the 3 μ L of click solution containing 1 μ L of CuBr solution (0.01 g of CuBr in 700 μ L of DMSO/t-BuOH in 3:1) and 2 μ L of TBTA ligand solution was added in the reaction mixture. The solution was purged with N₂ gas and shaken for 14 h in the dark at room temperature. To remove unreacted reactants from the reaction mixture, ethanol precipitation was performed, and the precipitant was dissolved in 15 μ L of water. The click product was analyzed and purified with the 12% denature PAGE gel (Figures SSA and S6A).

Synthesis of 3' Cholesterol-TEG-DNA. A solution of 2 μ L (250 μ M) of 5-octadiynyl deoxyuridine-modified DNA was mixed with 8 μ L (250 μ M) of azido-TEG-cholesterol. Then, the 3 μ L of click solution containing 1 μ L of CuBr solution (0.01 g of CuBr in 700 μ L of DMSO/t-BuOH in 3:1) and 2 μ L of TBTA ligand solution was added in the reaction mixture. The solution was purged with N₂ gas and shaken for 14 h in the dark at room temperature. To remove unreacted reactants from the reaction mixture, ethanol precipitation was performed, and the precipitant was dissolved in 15 μ L of water. The click product was analyzed and purified with the 15% denature PAGE gel (Figures S5B and S6B).

Synthesis of DNA Constructs for Single-Molecule Investigations. An oligo containing polythymine (T₄₀) was annealed with two oligos conjugated with a host molecule at the 5' end and a guest molecule at the 3' end. The annealed construct was phosphorylated and then ligated to the biotin-labeled 2028 bp and digoxigenin-labeled 2391 bp dsDNA handles (Figure S7). The 2028 bp DNA handle was synthesized from the polymerase chain reaction (PCR) of a pBR322 plasmid template by using two primers, 5'-biotin-TEG-GCA TTA GGA AGC AGC CCA GTA GTA GG 3' and 5' AAA ATC TAG AGG CTA CAC TAG AAG GAC AGT

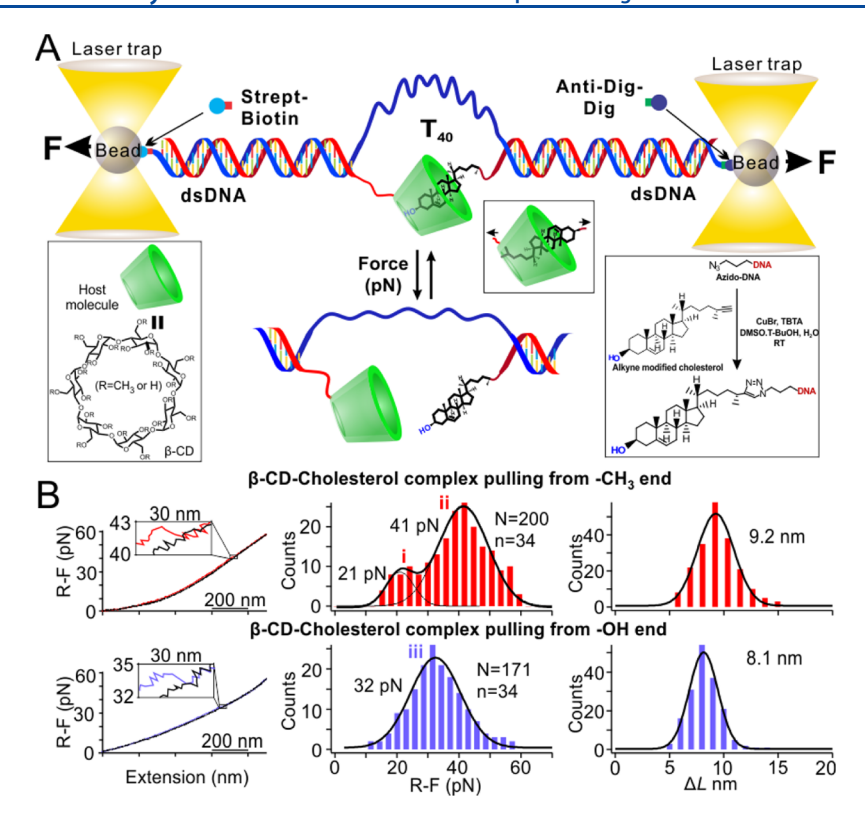


Figure 1. High-throughput single-molecule mechanical unfoldings for cholesterol and cyclodextrin host—guest complexes. (A) Experimental setup for the optical-tweezer experiment in which a β-cyclodextrin-cholesterol complex pulled from the alkyl end is shown. Right inset shows click-chemistry preparations for the cholesterol–DNA conjugates. The middle inset depicts the pulling of the complex from the hydroxyl end of cholesterol. Note cholesterol and cyclodextrin are located in different ssDNA strands. (B) Top: a typical force-extension curve, rupture force, and change-in-contour-length (ΔL) histogram for the β-CD-cholesterol complex pulled from the alkyl end of cholesterol. Bottom: a typical force-extension curve, rupture force, and change-in-contour-length (ΔL) histogram for the β-CD-cholesterol complex pulled from the hydroxy end of cholesterol. Note: the green barrel depicts methylated-β-CD (Me-β-CD) or β-CD. N and n represent total number of unfolding features and number of molecules, respectively.

ATT TG 3'. A sticky end compatible with the polyT containing fragments was generated by digesting the PCR-purified product using an XbaI enzyme. Similarly, PCR was performed to prepare the 2391 bp handle by using the λ-DNA template with two primers, 5' AAA AAA AAG AGC TCC TGA CGC TGG CAT TCG CAT CAA AG 3' and 5' AAA AAA AAG GTC TCG CCT GGT TGC GAG GCT TTG TGC TTC TC 3'. Then, the PCR product was digested by the SacI enzyme, which was followed by the labeling with digoxigenin-dUTP at the 3'-end SacI digested overhang by using terminal transferase for 8 h at 37 °C. By using the BsaI-HFv2 enzyme, the digoxigenin-labeled product was digested and purified, which generated an overhang that was compatible with the polyT-containing fragment.

Finally, using the T4 DNA ligase enzyme, the two dsDNA handles and the annealed polyT-containing fragment were ligated and stored in the $-20~^{\circ}\text{C}$ in 1 mM Tris-HCl buffer (pH 7.4) after the agarose gel purification.

Single-Molecule Force Ramping Experiments. A dual-beam laser-tweezer instrument was utilized to carry out single-molecule experiments. All the experiments were performed in a buffer containing 10 mM Tris and 100 mM KCl (pH 7.4) at 23 °C. Two types of polystyrene beads were used to capture the DNA construct. The DNA construct prepared above was incubated with streptavidin-coated polystyrene beads (diameter 1.87 μ m). The DNA-immobilized bead and the digoxigenin antibody-coated bead (diameter 2.1 μ m) were separately captured by two laser traps. By using affinity linkages of

streptavidin/biotin and digoxigenin/antibody-digoxigenin, the DNA construct was tethered between the two beads by bringing two beads in contact with each other. One of the laser foci was movable, while the other was fixed by controlling the laser beam's direction. The tethered DNA was stretched by moving the two beads away from each other. During the movement, the tension was produced on the host-guest complex, which was recorded as force-extension (F-X)curves via the LabView program (National Instruments, Austin, TX) at 1 kHz with a loading rate of 5.5 pN/s (in the 10-30 pN range) based on the displacement of the bead from the center of the trap (measured by position-sensitive photodetectors) and the spring constant of each trap (calibrated by the thermal motion of the bead in the trap). A single-molecule presence was confirmed by looking at the \sim 65 pN plateau at the F-X curve due to the phase transition of duplex DNA to a DNA form with unknown structures.³¹

The collected F-X curves were filtered through a Savitzky–Golay function with a time constant of 10 ms in the Matlab program (The MathWorks, Natick, MA), and the observed dissociation events in the F-X curves were used to determine the mechanical stability (rupture forces) of the host–guest interaction.

Change in Contour Length (ΔL). During the dissociation of a host–guest complex, the expected ΔL was calculated by the general eq 1

$$\Delta L = L - x \tag{1}$$

where L is the total contour length of 40T which can be determined as, $L = L_{\rm nt} \times 40$ nt = ~ 18 nm, where $L_{\rm nt}$ is the contour length of a single nucleotide, 0.40–0.45 nm/nt, $^{32-34}$ and x is the end-to-end distance. Given by the sum of the length of the 5' end linker (~ 1.7 nm), the length of the 3'-end linker (~ 4.7 nm), the length of cholesterol (~ 1.7 nm), 35 and the outer barrel diameter of the β -CD (~ 1.5 nm), this results in a total x of ~ 10 nm.

Therefore, the expected change-in-contour-length (ΔL) for a β -CD-cholesterol complex is $\sim (18-10)=8$ nm, which falls into the observations (see the rightmost histograms of Figures 1B and 4B).

Data Analysis. The extension difference between the stretching and the relaxing traces at a force (F) gives the change in extension (Δx) at that force. Then, the resulting Δx value at this force was converted to the change-in-contourlength (ΔL) by using a worm-like chain model (eq 2), 36,37 as follows

$$\Delta x/\Delta L = 1 - 1/2(k_B T/FP)1/2 + (F/S)$$
 (2)

where Δx is the change in the end-to-end distance (or extension) between the two optically trapped beads, ΔL is the change in contour length, $k_{\rm B}$ is the Boltzmann constant, T is the absolute temperature, P is the persistent length of dsDNA (50.8 nm), and S is the stretching modulus (1243 pN).

Molecular Simulation Methods. Nonequilibrium SMD simulations and umbrella sampling technique^{39,40} for free energy calculations were performed using the LAMMPS computational package.⁴¹ Detailed computational procedures are given in Supporting Information, Section S1. In single-molecule SMD simulations, the center of mass of the cyclodextrin molecule was fixed. The cholesterol molecule was connected to a driving spring to mimic the IMMF dissociation force measurement in the experiment. The spring was connected to the C3 atom of cholesterol (Figure 3A) to mimic the pulling from the hydroxyl head or to the C25 atom of cholesterol to mimic the pulling from the alkyl tail (Figure 3A). The pulling speed was 0.002 Å/ps.

The umbrella sampling technique ⁴⁰ was used for free energy calculations of the cyclodextrin—cholesterol complex in aqueous solution (Supporting Information, Section 2). The distance, d, between the center of mass of cyclodextrin and the C3/C25 of the cholesterol molecule (Figure 3A) was used as a single collective variable during the sampling. The free energy profile was calculated by $G(d) = -k_{\rm B}T \ln[P(d)]$, where $k_{\rm B}$ is the Boltzmann's constant, T is the temperature, and P(d) is the probability distribution.

RESULTS

Interaction between Cholesterol and β -CD is Dependent on Directions. To measure IMMFs in cholester-ol— β -CD interactions, we used a single-molecule DNA platform in optical tweezers to mechanically disassemble cyclodextrin—cholesterol host—guest complexes (Figure 1A). We first conjugated the azide-modified β -CD with an alkyne-modified ssDNA fragment (Figures S1—S4) and alkyne/azide-modified cholesterol with an azide/alkyne modified ssDNA fragment (Figures 1A (inset), S5, and S6) by copper-catalyzed cycloaddition reactions. Each host- or guest-conjugated oligonucleotide fragment was then hybridized with a polythymine (T40) containing DNA. The hybridized DNA was ligated with biotinylated 2028 bp and digoxigenin-labeled 2391 bp dsDNA handles (Figure S7). The DNA construct was

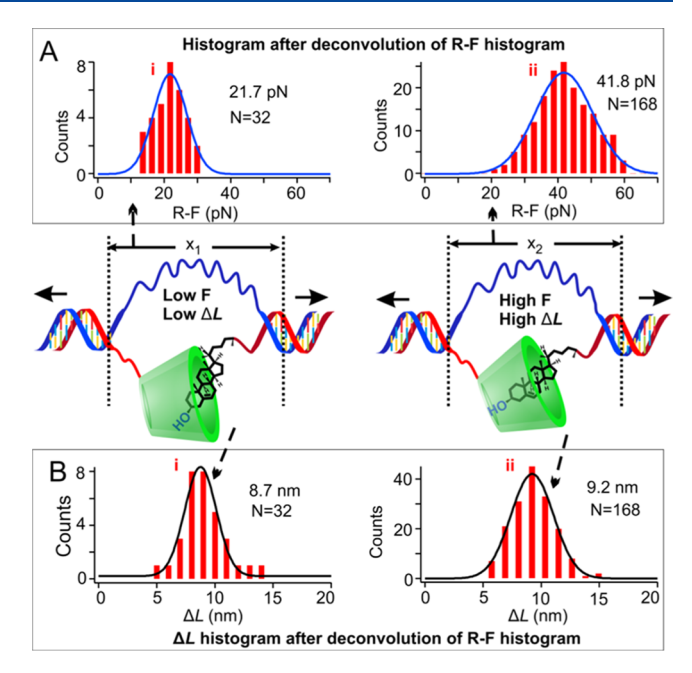


Figure 2. (A) Deconvoluted rupture force (R-F) histograms based on the Figure 1B (top) data (left: lower force population (i); right: higher force population (ii)). (B) Corresponding change-in-contourlength (ΔL) histograms (i and ii). The middle panels show possible interaction models for the β -CD and cholesterol complex pulled from the alkyl end of cholesterol. N represents total number of unfolding features.

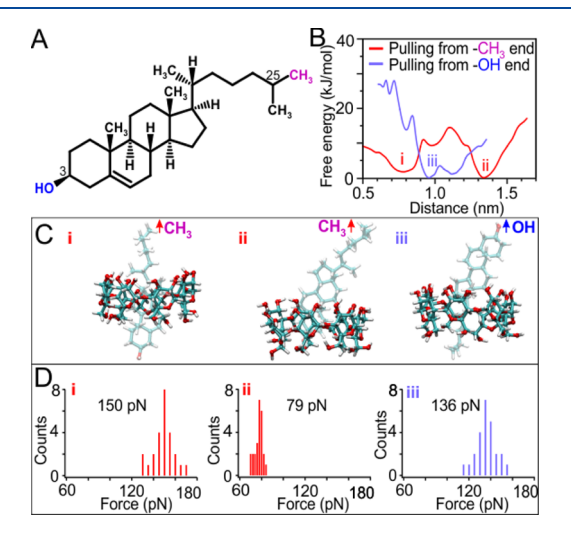


Figure 3. (A) Chemical structure of cholesterol. (B) Variations of the free energy versus the distance, d, between β -CD and cholesterol with different pulling directions. The distance, d, is defined as the length between the center of mass of β -CD and the 3rd (blue trace) or 25th carbon atom (red trace) on the cholesterol molecule, as shown in Figure 3A. (C i–iii), typical structures of the host–guest complexes near the free energy minima, corresponding to point i-iii in Figure 3B. Colors: red, O; white, H; light blue, C. Water molecules are not shown for clarity. (D i–iii), dissociation force histograms for the β -CD-cholesterol complex starting from the initial conformations corresponding to the free energy minima i, ii, and iii shown in Figure 3B, respectively. For each (meta)stable state, 25 independent SMD simulations are performed.

finally tethered between two optically trapped beads by using affinity linkages of streptavidin/biotin and digoxigenin/antibody (Figure 1A). The T_{40} linker was employed in the

molecular platform to facilitate repetitive assembly and disassembly of the cyclodextrin—cholesterol complex. After the complex was disassembled mechanically, the T40 linker would keep the host and guest molecules in proximity, enabling the facile reformation of the host—guest pair for the next round of experiments.

We started to evaluate mechanical association and dissociation of the β -CD-cholesterol complex at a loading rate of 5.5 pN/s by grabbing the cholesterol from its alkyl tail. After the β -CD-cholesterol complex was formed in the DNA tether between the two optically trapped beads, we moved one bead away from the other using a steerable mirror. This increased the tensile force in the DNA tether, which eventually breaks the β -CD-cholesterol complex, manifested as a rupture event in F-X curves (Figure 1B, top left). The tension inside the DNA construct did not relax to zero because of the T₄₀ linker connecting two dsDNA handles, which was a strong indication that the rupture occurred at the β -CD-cholesterol complex. After breakage events, we relaxed the tension in the DNA tether by moving the two optically trapped beads closer, during which the host-guest pair reformed for the next round of the mechanical unfolding procedure. From these repetitive rupture events, we plotted the unfolding force (i.e., IMMF: intermolecular mechanical force) histogram of the host-guest complex pulled from the alkyl end of the cholesterol. The histogram gave a minor population centered at 21 pN and a major population with an average force of 41 pN (Figure 1B, top middle). Such a result suggests that multiple binding complexes may exist due to the partial or complete insertion of cholesterol in the β -CD cavity. Next, we repeated the mechanical unfolding of the β -CD-cholesterol complex by pulling the hydroxyl head group of the cholesterol (Figure 1B, bottom) at the same loading rate of 5.5 pN/s in order to compare the complexation of the cholesterol with different cyclodextrin hosts, as well as the orientation effect under the same kinetic regime. We observed a single rupture force (IMMF) population at 32 pN.

From these two experiments, it is clear that the mechanical stability of the β -CD and cholesterol complex depends on the pulling orientation of the complex. At the time when cholesterol was pulled from the alkyl tail, the majority of the fused hydrophobic rings is buried inside the hydrophobic cavity of the β -CD. The relatively strong hydrophobic interaction therefore led to high mechanical stability (41 pN). 13,42 When the β -CD-cholesterol complex was pulled from the hydroxy head of the cholesterol, parts of the alkyl and fused rings were contained inside hydrophobic cavity. Because the alkyl chain has reduced hydrophobic interaction with the cyclodextrin cavity with respect to the fused rings due to its reduced interfacial area⁴³ and increased flexibility, the mechanical stability was reduced (32 pN). In both cases, we assume that the cholesterol molecule enters the β -CD hydrophobic cavity through its wide opening side (Figure 1A). 17,44-46 This will be further elaborated below.

To understand the low force population of the β -CD-cholesterol complex pulled from the alkyl tail (21 pN), we deconvoluted the force histogram into two populations centered at 22 pN and 42 pN using a randomized deconvolution method⁴⁷ (Figure 2A). Because each unfolding event yielded a value of change-in-contour-length (ΔL), we constructed two ΔL histograms corresponding to the two unfolding forces (Figure 2B). These ΔL values (8.7 nm and 9.2 nm) fell within the expected range with respect to the contour

length of the T_{40} linkage (see Figure S8 and Materials and Methods section for detailed calculation). We hypothesized that there were two configurations of the β -CD-cholesterol complex pulled from the alkyl tail of the cholesterol. While the lower ΔL value was likely due to the larger end-to-end distance (x_1) by the partial complexation of the cholesterol in the β -CD cavity (Figure 2B left), the higher ΔL value can be due to the complete insertion of the cholesterol in the β -CD cavity, which resulted in smaller end-to-end distance (x_2) (Figure 2B right).

To test this two-configuration hypothesis in the β -CDcholesterol complex pulled from the alkyl end, we performed nonequilibrium SMD simulation in conjunction with the umbrella sampling technique to obtain molecular insights into the structure-force relationship during this single-molecule IMMF spectroscopy measurement. Here, we assume that the cholesterol molecule always enters and then is pulled out of the cyclodextrin through its wide opening (Figures 1A and 3C). The umbrella sampling indeed showed a free energy profile with two energy minima [Figure 3B, d = 0.80 nm (state i) and d = 1.34 nm (state ii)] portraying two different (meta)stable configurations [Figure 3C(i,ii)], as revealed by other simulation studies. 25 A comparison of the end-to-end distance for these two configurations revealed a ~0.54 nm difference, which matched very well with the mechanical unfolding measurements of 0.5 nm (Figure 2B). However, for the β -CDcholesterol complex pulled from the hydroxyl end, the simulation showed a single energy valley at $d \sim 0.95$ nm (state iii). The second valley at $d \sim 1.1$ nm has an energy barrier less than $1k_BT$, indicating a single stable configuration of the host-guest complex. This result is in full agreement with the IMMF mechanical unfolding experiments.

We further performed extensive SMD simulations to measure the dissociation force of the β -CD and cholesterol complex pulled either from the alkyl tail or from the hydroxyl head passing through the wide opening of β -CD. Pulling from the alkyl tail showed two force spectroscopy populations [Figure 3D(i,ii)]. The snapshots of the molecular structures indicated that the higher force population corresponded to the fused rings of the cholesterol fully interacted with the hydrophobic cavity of the cyclodextrin. On the other hand, pulling from the hydroxyl head revealed only one rupture force population [Figure 3D(iii)]. In addition, the trend of the rupture forces retrieved from SMD simulations in all configurations/orientations of the host-guest complex gave a striking agreement with the mechanical unfolding experiments, though overall, the magnitudes of the simulated rupture forces were larger than the experimental values due to the very high pulling rate in SMD simulations, a well-known timescale issue

An interesting question concerning whether the cholesterol molecule should always enter and then be pulled out of the hydrophobic cavity of the cyclodextrin through its wide opening (the secondary hydroxyl rim of the β -CD exposing the -OH side) or the same procedure could also happen on the narrow opening side (the primary hydroxyl rim of the β -CD exposing the -CH₂OH side). Our extended free energy calculations of the cholesterol molecule passing through both openings (Figure S9), either by pulling from the alkyl end or from the hydroxyl end of the cholesterol, clearly show that a large free energy penalty (\sim 30 kJ/mol) will be encountered when passing through the narrow opening, compared to a relatively low free energy barrier (\sim 15 kJ/mol) when passing through the wide opening. This could be further illustrated by

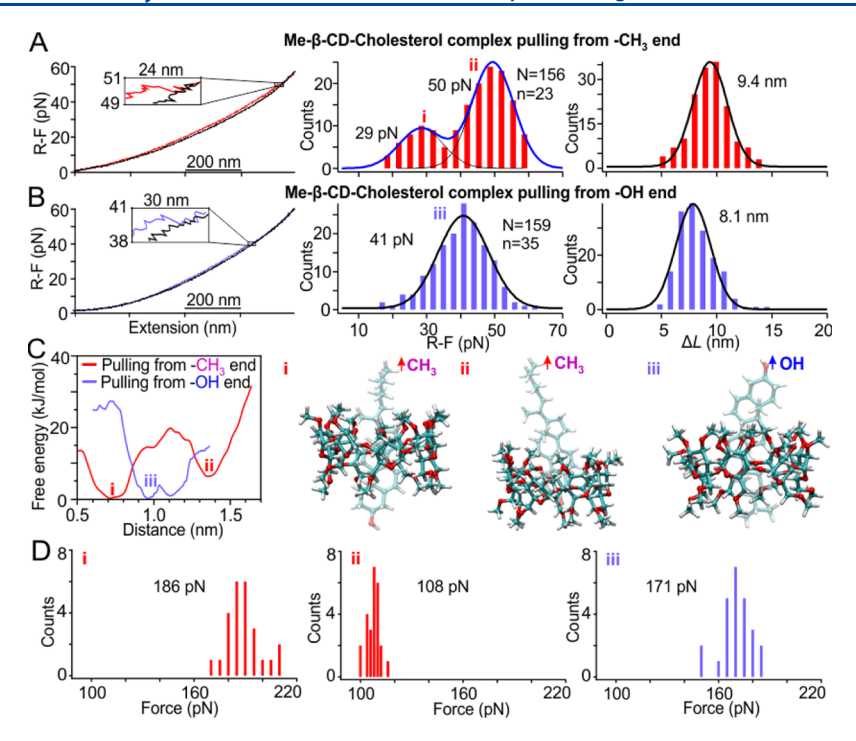


Figure 4. (A) Typical force-extension curve, rupture force, and change-in-contour-length (ΔL) histogram for the Me- β -CD-cholesterol complex pulled from the alkyl end of cholesterol. N and n represent total number of unfolding features and number of molecules, respectively. (B) Typical force-extension curve, rupture force, and change-in-contour-length (ΔL) histogram for the Me- β -CD-cholesterol complex pulled from the hydroxy end of cholesterol. (C) Variations of the free energy vs the distance, d, between Me- β -CD and cholesterol with different pulling directions. Molecular conformations i—iii show the host—guest complexes near the free energy minima, corresponding to points i—iii in Figure 4C. (D) Dissociation force histograms for the Me- β -CD-cholesterol complex starting from the initial configurations corresponding to the free energy minima i, ii, and iii, as shown in Figure 4C, respectively.

analyzing conformation changes in the β -CD—cholesterol complex when pulling from the hydroxyl end of cholesterol, as shown in Figure S10. As the cholesterol molecule passes through the narrow opening [Figure S10(A1,A2)], it is seen that the $-CH_2OH$ rim of the β -CD undergoes a significant expansion, resulting in enthalpy increase of the complex. At the same time, majority of the seven hydroxyl groups on the narrow opening side of the β -CD are forced to rotate toward outside, resulting in the entropy decrease of the β -CD. Both effects lead to a significant increase of the free energy of the β -CD-cholesterol complex. In contrast, as the cholesterol molecule passes through the wide opening [Figure S10-(B1,B2)], the size of the secondary hydroxyl rim of the β -CD has almost no change, with all the 14 hydroxyl groups on the wide opening side fluctuating randomly. Therefore, we conclude that it is more energetically favorable for the cholesterol molecule to enter the cavity of the β -CD through the wide opening in actual mechanical unfolding experiments.

Molecular Mechanism of the Interaction between Methylated β -CD and Cholesterol. It has been found that methylated β -CD is more effective to solubilize cholesterol. ^{8,49-51} To understand the molecular mechanism of this phenomenon, we repeated the unfolding experiments by using permethylated beta-cyclodextrin (Me- β -CD) as a host molecule. For this purpose, we incorporated the Me- β -CD-and alkyl tail-modified cholesterol at the 5' and 3' end of ssDNA, respectively, by using the construct preparing procedure as described above. After the mechanical unfolding of the Me- β -CD and the cholesterol complex pulled from the alkyl end of the cholesterol, we observed two IMMF populations (Figure 4A) similar to the β -CD case. We found

that the minor and the major force populations were centered at 29 and 50 pN, respectively, both of which were significantly higher than the corresponding populations in the β -CD case (22 and 42 pN, respectively, see Figure 1B, top middle panel).

Free energy calculations based on umbrella sampling for the pulling from the alkyl end of the cholesterol further confirmed the two different (meta)stable configurations separated by a much higher energy barrier, that is, ~20 kJ/mol in Figure 4C(i,ii) versus ~15 kJ/mol in Figure 3C(i,ii). In addition, our extensive SMD simulations revealed the third stable unfolding conformation, in which the cholesterol molecule adopted a direct parallel contact on the rim of the Me- β -CD. Pulling from the alkyl tail resulted in a continuous sliding of the molecule along the rim of the Me- β -CD (Figure S11A), which was not observed in the β -CD case. We anticipated this parallel pulling will give roughly the same rupture force comparable to the partially buried conformation, but the ΔL value is expected to be 2 nm greater than the partially buried conformation. Therefore, we did not count its contribution to the overall force. Interestingly, pulling from the hydroxyl head failed to give the parallel contact conformation. Instead, the flexible alkyl tail was readily trapped into the cavity of the Me- β -CD, resulting in a typical buried binding configuration [Figure 4C(iii)] that corresponds to the pulling of the hydroxyl head of the cholesterol. Compared to the β -CD case, we observed an overall increase of the rupture forces by \sim 25%. We attributed this force spectra increase to the larger hydrophobic cavity associated with the Me- β -CD than β -CD. The randomized deconvolution⁴⁷ of the IMMF unfolding force histogram in Figure 4A (middle panel) yielded two populations (Figure S12). The ΔL difference between these two species showed a

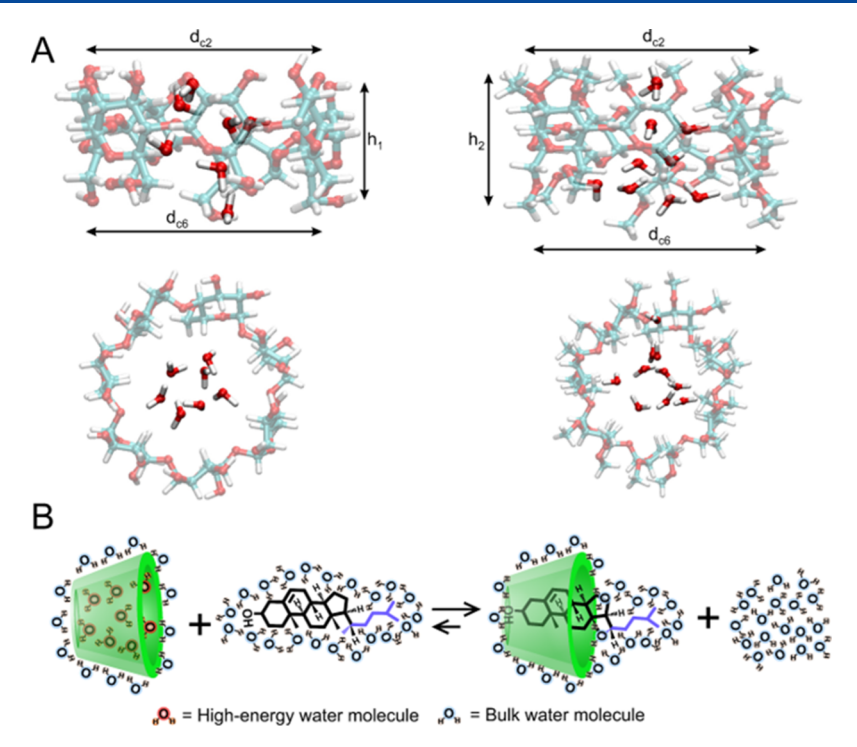


Figure 5. (A) Snapshots showing the structure of β -CDs (side view, upper left; top view, lower left) and Me- β -CD (right panels) with the average number of water molecules occupying their cavities. The upper/lower rim diameters and height of the cavity for each structure are also shown. The upper and lower rim diameters are evaluated using the C2 and C6 atoms in cyclodextrins, respectively. The height of the cavity is defined as the distance between the center of mass of O2 atoms and the center of mass of O6 atoms for β -CD and between the center of mass of carbon atoms in the upper CH3 groups and the lower CH3 groups for Me- β -CD. (B) Schematic diagram for the release of high energy water molecules upon β -CD-cholesterol complex formation.

value of 0.8 nm, which was largely consistent with SMD force spectroscopy simulations for the buried binding conformation (0.64 nm, between i and ii in Figure 4C).

We also investigated mechanical unfolding of the Me- β -CD and cholesterol complex pulled from the hydroxy head (-OH) of the cholesterol. Again, both single-molecule IMMF measurements (Figure 4B) and SMD force spectroscopy simulations [Figure 4C,D(iii)] showed a single population with increased mechanical stabilities compared to the β -CD [Figures 1B and 3C,D(iii)]. The striking agreement between the single-molecule unfolding and SMD simulation corroborated that both β -CD and Me- β -CD can interact with the cholesterol molecule in a direction-dependent manner. With respect to the β -CD, Me- β -CD has a cavity with increased hydrophobicity, which may explain their different interactions with the hydrophobic cholesterol guests.

To further explore the hydrophobic interaction between cholesterol guests and cyclodextrin hosts, we used equilibrium MD simulation to determine the number of high energy water molecules 19,52,53 displaced after the formation of the cholesterol-cyclodextrin complex. A geometry-based approach⁵⁴ was applied to count the number of water molecules inside the cavity. We found that 5-9 and 9-12 entrapped high-energy water molecules, with an average of 1.8 hydrogen bonds per water molecule, were released to the bulk from β -CD and Me- β -CD cavities, respectively (Figure 5A,B). The fact that Me- β -CD contains more high-energy water molecules was due to its larger cavity volume compared to the β -CD (Figure 5A, β -CD: upper rim diameter, 1.30 nm; lower rim diameter, 1.20 nm; and height of the cavity, 0.54 nm; Me-β-CD: upper rim diameter, 1.32 nm; lower rim diameter, 1.28 nm; and height of the cavity, 0.72 nm). These numbers are

consistent with other studies. S4-56 Detailed water hydration structures within β -CD and Me- β -CD are shown in Figure S13. The radius distribution functions for water molecules around the center of mass of β -CD/Me- β -CD are shown in Figure S14, in which the first peaks inside the cavities clearly show that Me- β -CD has a higher local density of water than β -CD. From these observations, it was evident that releasing the highenergy water molecules from the cyclodextrin cavity, together with "shearing off" the water molecules in the first hydration shell of the cholesterol molecule (15 \pm 4 H₂O molecules), is the driving force for the solubilization of cholesterols in cyclodextrins.

DISCUSSION

By using single-molecule force spectroscopy in optical tweezers, in combination with steered molecular dynamics simulations and umbrella sampling, we found that the IMMFs between cholesterols and cyclodextrins are orientation-dependent. The driving force for the solubilization of cholesterol molecules in cyclodextrins is the hydrophobic force which stemmed from the displacement of high-energy water molecules from cyclodextrin cavities.⁵³ From molecular simulations, we found that the cyclodextrin interacted with cholesterol better when the cholesterol molecule enters the wider opening of the cyclodextrin with the head-on (hydroxyl -OH group as the leading group) orientation. Such an orientation explains the facile removal of cholesterol guests in the phospholipid membrane by cyclodextrin hosts. It has been found that IMMF is 12-22 pN⁵⁷ when cholesterol molecules are pulled out of lipid membranes with a loading rate similar to that used in the optical-tweezer experiments here. This IMMF is lower than the IMMF (>30 pN) between the cyclodextrins and cholesterols measured in this work. Such an IMMF difference is in full agreement with the findings that β -CD is an excellent agent to extract cholesterol from cell membranes, which demonstrates that the IMMF can serve as a unique indicator for solubilities not only for cholesterols but also for other molecules.

The combined experimental/computational force spectroscopy studies described here also provide guidelines to facilitate the removal of cholesterol from the artery plaques, for example, by modification some of the hydroxyl groups in cyclodextrins with hydrophobic moieties. In addition, the measurement of IMMF can be used to evaluate and understand the solubility of guest molecules in host cavities, which have been exploited in host—guest systems for applications such as drug delivery and biosensing.

ASSOCIATED CONTENT

Supporting Information

The Supporting Information is available free of charge at https://pubs.acs.org/doi/10.1021/acs.jpcb.1c03916.

Molecular simulation methods, CD-DNA and cholesterol-DNA conjugate syntheses, and DNA construct preparation procedure for single-molecule force spectroscopy experiments, calculation for change-in-contourlength, free energy versus distance diagrams in different pulling directions, conformation changes of the β -CD molecule, parallel conformation of Me- β -CD and cholesterol, deconvoluted histograms for Me- β -CD and cholesterol pulling from the alkyl end (PDF), snap shots of water structures within CDs, and radial distribution functions of water oxygen around the cener of mass of CDs.

AUTHOR INFORMATION

Corresponding Authors

Yongsheng Leng — Department of Mechanical and Aerospace Engineering, The George Washington University, Washington, District of Columbia 20052, United States; ⊚ orcid.org/ 0000-0002-3558-5016; Email: leng@gwu.edu

Hanbin Mao – Department of Chemistry and Biochemistry, and Advanced Materials and Liquid Crystal Institute, Kent State University, Kent, Ohio 44242, United States;
ocid.org/0000-0002-6720-9429; Email: hmao@kent.edu

Authors

Shankar Pandey — Department of Chemistry and Biochemistry, and Advanced Materials and Liquid Crystal Institute, Kent State University, Kent, Ohio 44242, United States; orcid.org/0000-0001-5576-6714

Yuan Xiang — Department of Mechanical and Aerospace Engineering, The George Washington University, Washington, District of Columbia 20052, United States; orcid.org/ 0000-0002-4665-3360

Dilanka V. D. Walpita Kankanamalage – Department of Chemistry, Tulane University, New Orleans, Louisiana 70118, United States

Janarthanan Jayawickramarajah — Department of Chemistry, Tulane University, New Orleans, Louisiana 70118, United States; © orcid.org/0000-0001-5271-1523

Complete contact information is available at: https://pubs.acs.org/10.1021/acs.jpcb.1c03916

Author Contributions

S.P. and Y.X. contribute equally

Notes

The authors declare no competing financial interest.

ACKNOWLEDGMENTS

H.M. thanks NIH (R01 CA236350, for construct preparation) and NSF (CBET-1904921 for mechanical unfolding) for financial support. Y.L. thanks NSF grant (CBET-1817394) for the computational studies of membrane fouling and separations. J.J. acknowledges support from NSF grant CHE-2003879. Xiao Zhou and Pravin Pathak are thanked for providing the azido-modified beta-cyclodextrin analogues.

REFERENCES

- (1) Grebe, A.; Latz, E. Cholesterol crystals and inflammation. *Curr. Rheumatol. Rep.* **2013**, *15*, 313.
- (2) Simons, K.; Ehehalt, R. Cholesterol, lipid rafts, and disease. J. Clin. Invest. 2002, 110, 597–603.
- (3) Simons, K.; Toomre, D. Lipid rafts and signal transduction. *Nat. Rev. Mol. Cell Biol.* **2000**, *1*, 31–39.
- (4) Kim, H.; Han, J.; Park, J.-H. Cyclodextrin polymer improves atherosclerosis therapy and reduces ototoxicity. *J. Controlled Release* **2020**, 319, 77–86.
- (5) Mahjoubin-Tehran, M.; Kovanen, P. T.; Xu, S.; Jamialahmadi, T.; Sahebkar, A. Cyclodextrins: Potential therapeutics against atherosclerosis. *Pharmacol. Ther.* **2020**, 214, 107620.
- (6) Zimmer, S.; Grebe, A.; Bakke, S. S.; Bode, N.; Halvorsen, B.; Ulas, T.; Skjelland, M.; De Nardo, D.; Labzin, L. I.; Kerksiek, A.; et al. Cyclodextrin promotes atherosclerosis regression via macrophage reprogramming. *Sci. Transl. Med.* **2016**, *8*, 333ra50.
- (7) Braga, S. S. Cyclodextrins: Emerging Medicines of the New Millennium. *Biomolecules* **2019**, *9*, 801.
- (8) Christian, A. E.; Haynes, M. P.; Phillips, M. C.; Rothblat, G. H. Use of cyclodextrins for manipulating cellular cholesterol content. *J. Lipid Res.* **1997**, *38*, 2264–2272.
- (9) Deng, W.; Bukiya, A. N.; Rodríguez-Menchaca, A. A.; Zhang, Z.; Baumgarten, C. M.; Logothetis, D. E.; Levitan, I.; Rosenhouse-Dantsker, A. Hypercholesterolemia Induces Up-regulation of KACh Cardiac Currents via a Mechanism Independent of Phosphatidylinositol 4,5-Bisphosphate and $G\beta\gamma^*$. *J. Biol. Chem.* **2012**, 287, 4925–4935.
- (10) Slayden, A.; North, K.; Bisen, S.; Dopico, A. M.; Bukiya, A. N.; Rosenhouse-Dantsker, A. Enrichment of Mammalian Tissues and Xenopus Oocytes with Cholesterol. *J. Visualized Exp.* **2020**, *157*, No. e60734.
- (11) Best, R. B.; Paci, E.; Hummer, G.; Dudko, O. K. Pulling Direction as a Reaction Coordinate for the Mechanical Unfolding of Single Molecules. *J. Phys. Chem. B* **2008**, *112*, 5968–5976.
- (12) Sun, Y.; Di, W.; Li, Y.; Huang, W.; Wang, X.; Qin, M.; Wang, W.; Cao, Y. Mg2+-Dependent High Mechanical Anisotropy of Three-Way-Junction pRNA as Revealed by Single-Molecule Force Spectroscopy. *Angew. Chem., Int. Ed.* **2017**, *56*, 9376–9380.
- (13) López, C. A.; de Vries, A. H.; Marrink, S. J. Molecular Mechanism of Cyclodextrin Mediated Cholesterol Extraction. *PLoS Comput. Biol.* **2011**, *7*, No. e1002020.
- (14) Schönherr, H.; Beulen, M. W. J.; Bügler, J.; Huskens, J.; van Veggel, F. C. J. M.; Reinhoudt, D. N.; Vancso, G. J. Individual Supramolecular Host—Guest Interactions Studied by Dynamic Single Molecule Force Spectroscopy. *J. Am. Chem. Soc.* **2000**, *122*, 4963—4967.
- (15) Auletta, T.; de Jong, M. R.; Mulder, A.; van Veggel, F. C. J. M.; Huskens, J.; Reinhoudt, D. N.; Zou, S.; Zapotoczny, S.; Schönherr, H.; Vancso, G. J.; et al. β -Cyclodextrin Host–Guest Complexes Probed under Thermodynamic Equilibrium: Thermodynamics and AFM Force Spectroscopy. *J. Am. Chem. Soc.* **2004**, *126*, 1577–1584.

- (16) Neuman, K. C.; Nagy, A. Single-molecule force spectroscopy: optical tweezers, magnetic tweezers and atomic force microscopy. *Nat. Methods* **2008**, *5*, 491–505.
- (17) Schönbeck, C. Charge Determines Guest Orientation: A Combined NMR and Molecular Dynamics Study of β -Cyclodextrins and Adamantane Derivatives. *J. Phys. Chem. B* **2018**, *122*, 4821–4827.
- (18) Sadlej-Sosnowska, N.; Kozerski, L.; Bednarek, E.; Sitkowski, J. Fluorometric and NMR Studies of the Naproxen-Cyclodextrin Inclusion Complexes in Aqueous Solutions. *J. Inclusion Phenom. Macrocycl. Chem.* **2000**, *37*, 383–394.
- (19) Connors, K. A. The Stability of Cyclodextrin Complexes in Solution. *Chem. Rev.* **1997**, 97, 1325–1358.
- (20) Isralewitz, B.; Gao, M.; Schulten, K. Steered molecular dynamics and mechanical functions of proteins. *Curr. Opin. Struct. Biol.* **2001**, *11*, 224–230.
- (21) Park, S.; Khalili-Araghi, F.; Tajkhorshid, E.; Schulten, K. Free energy calculation from steered molecular dynamics simulations using Jarzynski's equality. *J. Chem. Phys.* **2003**, *119*, 3559–3566.
- (22) Park, S.; Schulten, K. Calculating potentials of mean force from steered molecular dynamics simulations. *J. Chem. Phys.* **2004**, *120*, 5946–5961.
- (23) Xiang, Y.; Liu, Y.; Mi, B.; Leng, Y. Hydrated Polyamide Membrane and Its Interaction with Alginate: A Molecular Dynamics Study. *Langmuir* **2013**, *29*, 11600–11608.
- (24) Hayashino, Y.; Sugita, M.; Arima, H.; Irie, T.; Kikuchi, T.; Hirata, F. Predicting the Binding Mode of 2-Hydroxypropyl-β-cyclodextrin to Cholesterol by Means of the MD Simulation and the 3D-RISM-KH Theory. *J. Phys. Chem. B* **2018**, *122*, 5716–5725.
- (25) Yu, Y.; Chipot, C.; Cai, W.; Shao, X. Molecular Dynamics Study of the Inclusion of Cholesterol into Cyclodextrins. *J. Phys. Chem. B* **2006**, *110*, 6372–6378.
- (26) López, C. A.; de Vries, A. H.; Marrink, S. J. Computational microscopy of cyclodextrin mediated cholesterol extraction from lipid model membranes. *Sci. Rep.* **2013**, *3*, 2071.
- (27) Barrow, S. J.; Kasera, S.; Rowland, M. J.; del Barrio, J.; Scherman, O. A. Cucurbituril-Based Molecular Recognition. *Chem. Rev.* **2015**, *115*, 12320–12406.
- (28) Masson, E.; Raeisi, M.; Kotturi, K. Kinetics Inside, Outside and Through Cucurbiturils. *Isr. J. Chem.* **2018**, *58*, 413–434.
- (29) Pathak, P.; Yao, W.; Hook, K. D.; Vik, R.; Winnerdy, F. R.; Brown, J. Q.; Gibb, B. C.; Pursell, Z. F.; Phan, A. T.; Jayawickramarajah, J. Bright G-Quadruplex Nanostructures Functionalized with Porphyrin Lanterns. *J. Am. Chem. Soc.* **2019**, *141*, 12582–12591.
- (30) Pandey, S.; Kankanamalage, D. V. D. W.; Zhou, X.; Hu, C.; Isaacs, L.; Jayawickramarajah, J.; Mao, H. Chaperone-Assisted Host—Guest Interactions Revealed by Single-Molecule Force Spectroscopy. *J. Am. Chem. Soc.* **2019**, *141*, 18385–18389.
- (31) Smith, S. B.; Cui, Y.; Bustamante, C. Overstretching, B-DNA The elastic response of individual double-stranded and single-stranded DNA molecules. *Science* **1996**, *271*, 795–799.
- (32) Yu, Z.; Schonhoft, J. D.; Dhakal, S.; Bajracharya, R.; Hegde, R.; Basu, S.; Mao, H. ILPR G-Quadruplexes Formed in Seconds Demonstrate High Mechanical Stabilities. *J. Am. Chem. Soc.* **2009**, 131, 1876–1882.
- (33) Mills, J. B.; Vacano, E.; Hagerman, P. J. Flexibility of single-stranded DNA: use of gapped duplex helices to determine the persistence lengths of Poly(dT) and Poly(dA) 1 1Edited by B. Honig. *J. Mol. Biol.* 1999, 285, 245–257.
- (34) Tinland, B.; Pluen, A.; Sturm, J.; Weill, G. Persistence Length of Single-Stranded DNA. *Macromolecules* **1997**, *30*, *5763*–*5765*.
- (35) Hosta-Rigau, L.; Zhang, Y.; Teo, B. M.; Postma, A.; Städler, B. Cholesterol a biological compound as a building block in bionanotechnology. *Nanoscale* **2013**, *5*, 89–109.
- (36) Baumann, C. G.; Smith, S. B.; Bloomfield, V. A.; Bustamante, C. Ionic effects on the elasticity of single DNA molecules. *Proc. Natl. Acad. Sci. U.S.A.* **1997**, *94*, 6185–6190.
- (37) Yu, Z.; Mao, H. Non-B DNA Structures Show Diverse Conformations and Complex Transition Kinetics Comparable to

- RNA or Proteins-A Perspective from Mechanical Unfolding and Refolding Experiments. *Chem. Rec.* **2013**, *13*, 102–116.
- (38) Dhakal, S.; Cui, Y.; Koirala, D.; Ghimire, C.; Kushwaha, S.; Yu, Z.; Yangyuoru, P. M.; Mao, H. Structural and mechanical properties of individual human telomeric G-quadruplexes in molecularly crowded solutions. *Nucleic Acids Res.* **2013**, *41*, 3915–3923.
- (39) Kumar, S.; Rosenberg, J. M.; Bouzida, D.; Swendsen, R. H.; Kollman, P. A. THE weighted histogram analysis method for free-energy calculations on biomolecules. I. The method. *J. Comput. Chem.* **1992**, *13*, 1011–1021.
- (40) Torrie, G. M.; Valleau, J. P. Nonphysical sampling distributions in Monte Carlo free-energy estimation: Umbrella sampling. *J. Comput. Phys.* **1977**, 23, 187–199.
- (41) Plimpton, S. Fast Parallel Algorithms for Short-Range Molecular Dynamics. *J. Comput. Phys.* **1995**, *117*, 1–19.
- (42) Bonnet, P.; Jaime, C.; Morin-Allory, L. Structure and Thermodynamics of α -, β -, and γ -Cyclodextrin Dimers. Molecular Dynamics Studies of the Solvent Effect and Free Binding Energies†. *J. Org. Chem.* **2002**, *67*, 8602–8609.
- (43) Silberberg, M. S. Principles of General Chemistry; McGraw-Hill: New York, 2013.
- (44) Vander Heyden, Y.; Mangelings, D.; Matthijs, N.; Perrin, C. 18-Chiral Separations. In *Separation Science and Technology*; Ahuja, S., Dong, M. W., Eds.; Academic Press, 2005; Vol. 6, pp 447–498. DOI: 10.1016/s0149-6395(05)80062-5
- (45) Ravichandran, R.; Divakar, S. Inclusion of Ring A of Cholesterol Inside the β -Cyclodextrin Cavity: Evidence from Oxidation Reactions and Structural Studies. *J. Inclusion Phenom. Mol. Recognit. Chem.* **1998**, 30, 253–270.
- (46) Nishijo, J.; Moriyama, S.; Shiota, S. Interactions of Cholesterol with Cyclodextrins in Aqueous Solution. *Chem. Pharm. Bull.* **2003**, *51*, 1253–1257.
- (47) Dhakal, S.; Schonhoft, J. D.; Koirala, D.; Yu, Z.; Basu, S.; Mao, H. Coexistence of an ILPR i-Motif and a Partially Folded Structure with Comparable Mechanical Stability Revealed at the Single-Molecule Level. *J. Am. Chem. Soc.* **2010**, *132*, 8991–8997.
- (48) Li, P. C.; Makarov, D. E. Theoretical Studies of the Mechanical Unfolding of the Muscle Protein Titin: Bridging the Time-Scale Gap between Simulation and Experiment. *J. Chem. Phys.* **2003**, *119*, 9260–9268.
- (49) Kilsdonk, E. P. C.; Yancey, P. G.; Stoudt, G. W.; Bangerter, F. W.; Johnson, W. J.; Phillips, M. C.; Rothblat, G. H. Cellular cholesterol efflux mediated by cyclodextrins. *J. Biol. Chem.* **1995**, 270, 17250–17256.
- (50) Atger, V. M.; de la Llera Moya, M.; Stoudt, G. W.; Rodrigueza, W. V.; Phillips, M. C.; Rothblat, G. H. Cyclodextrins as catalysts for the removal of cholesterol from macrophage foam cells. *J. Clin. Invest.* **1997**, *99*, 773–780.
- (51) Zidovetzki, R.; Levitan, I. Use of cyclodextrins to manipulate plasma membrane cholesterol content: evidence, misconceptions and control strategies. *Biochim. Biophys. Acta* **2007**, *1768*, 1311–1324.
- (52) Biedermann, F.; Nau, W. M.; Schneider, H.-J. The Hydrophobic Effect Revisited-Studies with Supramolecular Complexes Imply High-Energy Water as a Noncovalent Driving Force. *Angew. Chem., Int. Ed.* **2014**, *53*, 11158–11171.
- (53) Biedermann, F.; Uzunova, V. D.; Scherman, O. A.; Nau, W. M.; De Simone, A. Release of High-Energy Water as an Essential Driving Force for the High-Affinity Binding of Cucurbit[n]urils. *J. Am. Chem. Soc.* **2012**, *134*, 15318–15323.
- (54) Sandilya, A. A.; Natarajan, U.; Priya, M. H. Molecular View into the Cyclodextrin Cavity: Structure and Hydration. *ACS Omega* **2020**, *5*, 25655–25667.
- (55) Cézard, C.; Trivelli, X.; Aubry, F.; Djedaïni-Pilard, F.; Dupradeau, F.-Y. Molecular dynamics studies of native and substituted cyclodextrins in different media: 1. Charge derivation and force field performances. *Phys. Chem. Chem. Phys.* **2011**, *13*, 15103–15121.
- (56) Saenger, W.; Jacob, J.; Gessler, K.; Steiner, T.; Hoffmann, D.; Sanbe, H.; Koizumi, K.; Smith, S. M.; Takaha, T. Structures of the

Common Cyclodextrins and Their Larger AnaloguesBeyond the Doughnut. *Chem. Rev.* **1998**, 98, 1787–1802. (57) Stetter, F. W. S.; Cwiklik, L.; Jungwirth, P.; Hugel, T. Single lipid extraction: the anchoring strength of cholesterol in liquidordered and liquid-disordered phases. Biophys. J. 2014, 107, 1167-